

# A device for stereotaxic viral delivery into the brains of neonatal mice

Pedro R Olivetti<sup>1</sup> , Clay O Lacefield<sup>3</sup> & Christoph Kellendonk<sup>\*,1,2,3</sup> 

<sup>1</sup>Department of Psychiatry, Columbia University, 1051 Riverside Drive, New York, NY 10032, USA; <sup>2</sup>Department of Pharmacology, Columbia University Vagelos College of Physicians and Surgeons, 630 West 168th Street, 7th Floor, New York, NY 10032, USA; <sup>3</sup>Department of Neuroscience, New York State Psychiatric Institute, 1051 Riverside Drive, New York, NY 10032, USA; \*Author for correspondence: ck491@cumc.columbia.edu

BioTechniques 69: 307–312 (October 2020) 10.2144/btn-2020-0050

First draft submitted: 19 April 2020; Accepted for publication: 6 July 2020; Published online: 11 August 2020

## ABSTRACT

The increasing interest in manipulating neural circuits in developing brains has created a demand for reliable and accurate methods for delivering viruses to newborn mice. Here we describe a novel 3D-printed mouse neonatal stereotaxic adaptor for intracerebral viral injection that provides enhanced precision and reliability. Using this device, we injected *A2a-Cre* mice with a *Cre*-dependent hM4D-mCherry viral construct at postnatal day 1 (P1) and demonstrated selective expression in the striatal indirect pathway neurons on days P7, P11 and P25. Similarly, dopaminergic mid-brain neurons were selectively targeted with a *Cre*-dependent green fluorescent protein virus in *Dat-IRES-Cre* neonates and expression examined at P25. Our open-source neonatal stereotaxic mouse adaptor facilitates neonatal neuronal targeting, which should improve the ability to label and modify neural circuits in developing mouse brains.

## METHOD SUMMARY

The neonatal mouse stereotaxic adaptor, designed and easily 3D printed in-house, was fitted into the ear and tooth bars of a mouse digital stereotaxic apparatus and held the head of the ice-anesthetized newborn pups in a cone-shaped cradle during the virus injection procedure. After the secured heads were balanced on the AP and ML axes by adjusting the ear and tooth bars, *Cre*-dependent viruses (AAV5-hSyn-DIO-hM4D-mCherry or AAV5-hSyn-DIO-GFP) were injected to the desired brain region of *Cre*-expressing transgenic mice, while the animals were partially covered in ice. After completion of each surgery, the neonate was removed from the adaptor and returned to the den for recovery. Neuroanatomical viral expression was verified by immunofluorescence 6, 10 and 24 days after the procedure.

## KEYWORDS:

adaptor • neonatal mouse • stereotaxic • viral delivery • virus

Interest in neurodevelopmental disorders has grown significantly in recent years. The succession of critical or sensitive periods throughout postnatal development, during which neurons migrate, networks are assembled and synapses are formed, represents one of the most dynamic phases in the life of the mammalian brain [1–3]. Governed by intrinsic genetically encoded programs, activity-dependent factors and external inputs, these developmentally sensitive periods define the long-term characteristics of neuronal populations; early-life insults and genetic disruptions can leave long-lasting, deleterious imprints on key neuronal networks in the brain, with maladaptive functional consequences [4–7]. To understand the contributions of these early-life factors to disorders that are often not manifested until adulthood, the ability to selectively manipulate and/or measure the expression of genes and neuronal activity during early postnatal development has become a critical experimental need. In adult mice, stereotaxic injections of viral vectors have become routine in many neuroscience laboratories. However, the soft skulls of newborn mice preclude fixing their heads within conventional stereotaxic apparatuses. In addition, publicly available methods for injecting viruses in mouse neonates do not include mechanisms for precisely positioning the animal's head and often require the experimenter to hold the head manually during the injection [8–11]. These limitations may result in off-target viral delivery and restrict the use of these techniques to relatively large, easy-to-target brain regions.

Here we describe an adaptor for stereotaxic intracerebral viral delivery to neonatal mouse pups that provides precision and reliability even in small and deep regions. Designed and 3D printed in-house, the adaptor easily fits into the ear and tooth bars of an adult digital stereotaxic apparatus, allowing use of this device's precise positioning system along with the additional stability for the neonatal mouse provided by our adaptor. The dimensions of the adaptor are  $57 \times 25 \times 2$  mm, with an elevated 'step' where the horizontal cone-shaped head cradle rests. The lowest point of the head cradle stands at 9 mm from the base. At its widest point the cone diameter measures 7 mm. The top half of the cone is open, except for the nose arch that restricts head movements during the procedure. Circular holes (2 mm wide) on each side of the 'step' provide insertion points for securing the adaptor to the stereotaxic ear and tooth bars (Figure 1). A small piece of cloth tape secures the posterior aspect of the head to the cradle, eliminating the need for direct manual adjustments of head placement during the procedure (Figure 2). The adaptor was designed using TinkerCAD [12] free online design tool (an stl file with

# Benchmark

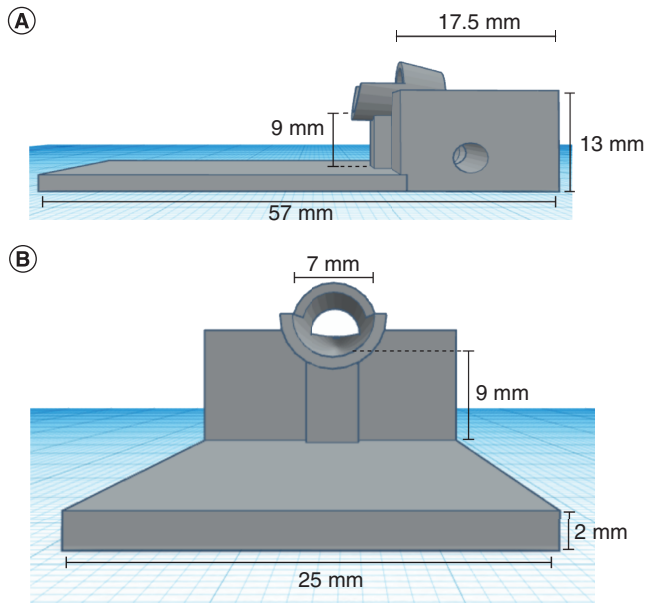


**Figure 1. Schematic diagram of neonatal stereotaxic adaptor. (A)** Side view of adaptor highlighting its length (57 mm), the base thickness (2 mm) and the height of the head 'step' at 17 mm. The profile of the head cradle is shown with the nose arch at the highest point of the diagram. Also visible is the right-side ear bar insert hole for mounting the adaptor on the stereotaxic frame. **(B)** Frontal view of the same diagram, highlighting the front opening of the head cradle with the nose arch in the background.

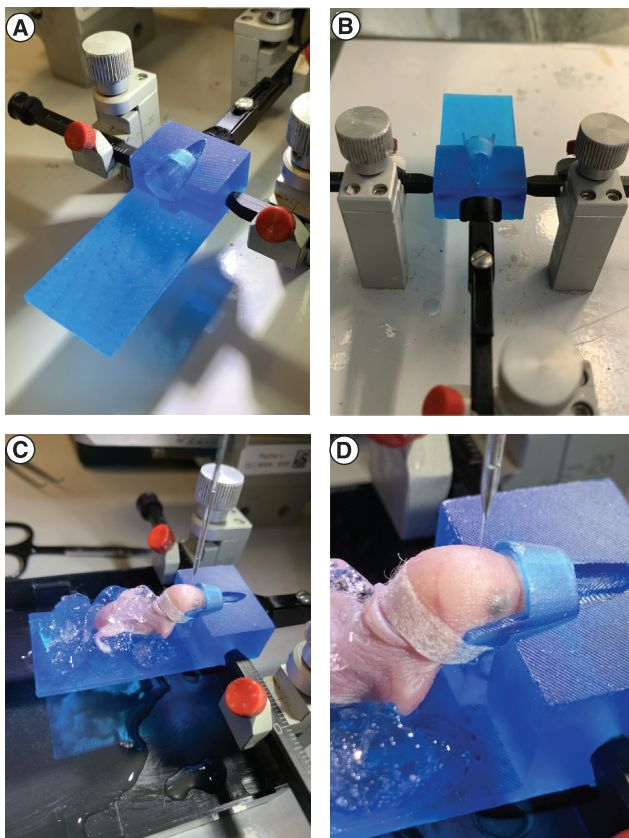


**Figure 2. The neonatal stereotaxic adaptor. (A & B)** Oblique and posterior views of the adaptor mounted on a stereotaxic frame. Note the placement of the two ear bars and the tooth bar in (B). **(C)** An anesthetized mouse neonate aged P1 resting on the adaptor with its head secured by tape and body partially covered by ice. **(D)** Detail of head placement in the cradle and cloth tape around the posterior aspect of the head. Also visible is a glass capillary needle inserted in the brain, going through the skin. The injection needle is attached to a Nanoject II mounted to the stereotaxic arm (not shown)..

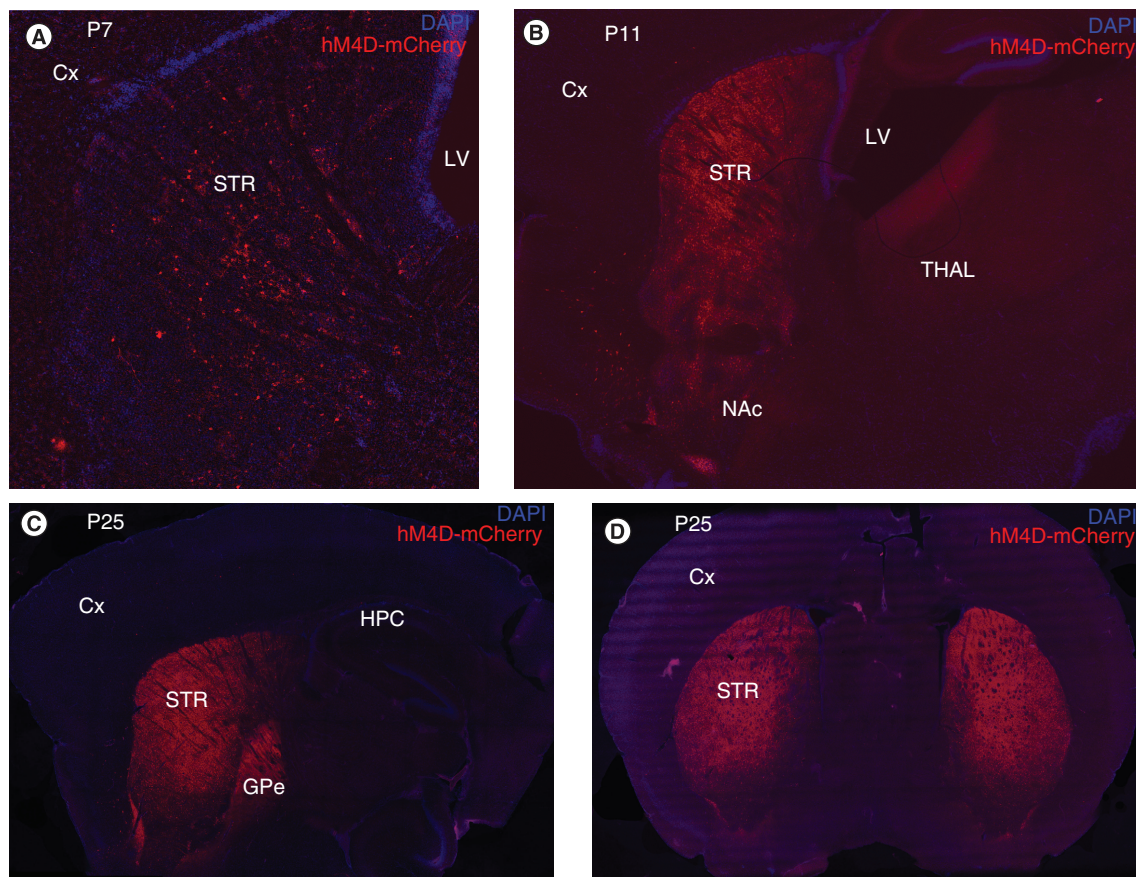


**Figure 3. Selective striatal indirect pathway viral expression.** (A) 5× epifluorescence sagittal brain section of a P7 *A2a-Cre* mouse injected with AAV5-hSyn-DIO-hM4D-mCherry at P1. *Cre*-driven expression of hM4D-mCherry is present at P7. No gross tissue damage is noticeable. (B) 2.5× epifluorescence sagittal brain section of a P11 *A2a-Cre* mouse injected with AAV5-hSyn-DIO-hM4D-mCherry at P1, illustrating the increase in viral expression. (C) 10× confocal image showing a sagittal brain section from a P25 *A2a-Cre* mouse injected with AAV5-hSyn-DIO-hM4D-mCherry at P1 using the neonatal adaptor. The robust red fluorescent signal is largely restricted to the dorsal striatum, with axonal projections shown at the globus pallidus pars externa. (D) 10× confocal coronal view of another P25 *A2a-Cre* mouse bilaterally injected at P1, highlighting the symmetry and striatal restriction of hM4D-mCherry expression. Primary antibody: rabbit anti-DsRed primary antibody (1:1000 dilution) targeting mCherry protein. Secondary antibody: chicken anti-rabbit Alexa Fluor 594 (1:1000 dilution).

Cx: Cortex; GPe: Globus pallidus pars externa; HPC: Hippocampus; LV: Lateral ventricle; NAc: Nucleus accumbens; STR: Striatum.

the necessary instruction for 3D printing is available in the Supplementary data) and fabricated in a high-resolution Form 2 3D printer with Draft Photopolymer resin (Formlabs, MA, USA) at an estimated cost of \$8–10 per device printed. In our experience, lower resolution 3D printing may not work well because the nose arch and other overhanging curved structures tend to collapse.

The protocol for using the adaptor to inject *Cre*-dependent viruses into the striatum and midbrain is described in detail in our separate protocol. Briefly, the adaptor is fixed to the ear and tooth bars, then a postnatal day 1 (P1) pup anesthetized by hypothermia is placed in the adaptor with the head carefully wedged in the head cradle and secured with a small piece of cloth tape (Figure 2C & D). After the head has been balanced using the stereotaxic frame, the target coordinates are determined in reference to the lambda skull suture using the same needle that will deliver the virus. The coordinates provided in this protocol are specific for the defined age of P1 and were adapted from the Developmental Mouse Atlas [13]. The device was designed to fit a P0–1 C57BL/6 neonate; older mice might not fit properly, thus we recommend empirical verification of regional targeting when using the device. In this protocol a Nanoject II nanoliter injector is used, but other methods for delivering viruses may be adapted. The glass needle (40–50 μm in diameter at the tip) is carefully pushed directly against the skin at the target location until the skull is perforated, then lowered to the desired depth calculated from the skin surface (Figure 2D). Delivery of the virus in each site can take place within 2 min, after which the needle is removed slowly at 0.05 mm/s, and the pup is transferred back to the den for recovery.

Two *Cre* recombinase mouse lines were used to demonstrate the advantages of the neonatal stereotaxic apparatus for targeting genetically specified neuronal populations in deep brain regions: *A2a-Cre* and *Dat-IRES-Cre* (IRES, internal ribosomal entry site). The

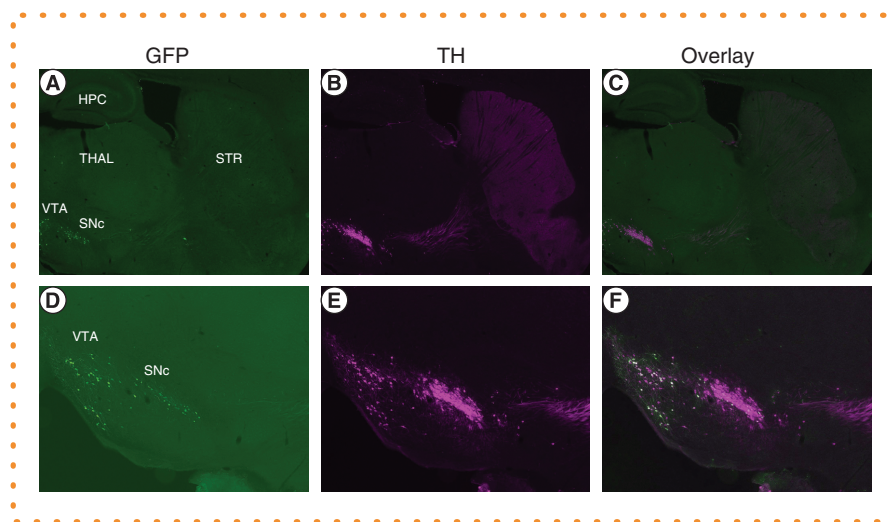


**Figure 4. Selective viral expression of GFP in midbrain dopaminergic neurons.** (A–C) Low magnification (2.5×) sagittal immunofluorescent view of a P25 *Dat-IRES-Cre* mouse injected at P1 with AAV5-hSyn-DIO-GFP virus. (A) Green immunofluorescent signal in VTA and SNc neurons illustrates selective targeting of dopamine neurons. (B) Immunostaining of TH-positive neurons. (C) Overlay of images in (A & B). (D–F) 5× magnification sagittal view of the same section highlighting the overlap of GFP (green) and TH (magenta) immunostaining in the VTA and SNc. Primary antibodies: chicken anti-GFP (1:1000) and mouse anti-TH (1:1000). Secondary antibodies: goat anti-chicken Alexa Fluor 488 (1:1000) and rabbit anti-mouse Alexa Fluor 546 (1:500).

GFP: Green fluorescent protein; HPC: Hippocampus; SNc: Substantia nigra pars compacta; STR: Striatum; TH: Tyrosine hydroxylase; THAL: Thalamus; VTA: Ventral tegmental area.

adenosine 2a receptor (A2a) is selectively expressed in the indirect pathway striatal medium spiny neurons starting on day P4 and is widely used as a marker to target this neuronal population [14,15]. The dopamine transporter protein (DAT) is selectively expressed as early as E18.5 by dopaminergic neurons of the midbrain ventral tegmental area (VTA) and substantia nigra pars compacta (SNc) [15–17]. *A2a-Cre* mice were injected bilaterally in the striatum with AAV5-hSyn-DIO-hM4D-mCherry on day P1 at two different positions along the Z-axis on the stereotaxic apparatus. This was done to achieve viral expression in both ventral and dorsal striatum, not to generate spatially separate expression between dorsal and ventral injections. The VTA/SNc region of *Dat-IRES-Cre* neonates was injected at P1 with AAV5-hSyn-DIO-GFP. Coordinates were derived from the vascular lambda, which corresponds to the skull lambda in neonates [18]. Postsurgical survival with this technique was 91.6%; in a cohort of 12 pups from four different litters, one did not recover. *A2a-Cre* mice were perfused at P7, P11 and P25, followed by routine immunohistochemistry to detect mCherry. Figure 3 shows representative images of the robust and selective expression of hM4D-mCherry in the indirect pathway medium spiny neurons in dorsal and ventral striatum, including projection fibers to the globus pallidus pars externa, at P7, P11 and P25. There was no noticeable tissue damage from the surgery at either P7, P11 or P25 (Figure 3). All tested brains showed correct targeting of the striatum with almost no expression detected outside of the striatum. Because *A2a-Cre* mice express *Cre* in the cortex and hippocampus [19], the striatum-selective expression of hM4D-mCherry demonstrates targeting-specificity of the viral injections at P1.

Targeting smaller regions in neonates poses a significant challenge, even with the support of Cre recombinase to restrict gene expression, because the injection could easily miss the region of interest, resulting in suboptimal or off-target expression. To demonstrate the capability of the neonatal adaptor to accurately target small and deep brain regions, *Dat-IRES-Cre* neonates (P1) were injected with AAV5-hSyn-DIO-GFP in the VTA/SNc region bilaterally. At P25 *Dat-IRES-Cre* mice were perfused and expression of green fluorescent protein (GFP) was verified by routine immunohistochemistry. No postsurgical deaths were recorded in a cohort of eight mice from two different litters. Five of the eight virus-injected *Dat-IRES-Cre* mice (62.5%) displayed selective expression of GFP in dopaminergic neurons located in the VTA/SNc region (Figure 4). The number of GFP-positive neurons in the VTA/SNc (pooled from three nonconsecutive sections per mouse and counted with ImageJ Particle Analyzer function) was  $99.4 \pm 32.8$  (mean  $\pm$  SD;  $n = 5$  mice). Two mice were costained for tyrosine hydroxylase (TH), a marker for dopaminergic neurons;  $32.8 \pm 1.6\%$  of TH-positive (dopaminergic) neurons displayed colocalization with GFP. Increasing the titer or changing the serotype may result in a greater percentage of TH-positive neurons infected with the virus [17].

The neonatal stereotaxic mouse adaptor is an easy-to-use tool for reliable, selective targeting of neuronal populations in the brains of newborn mice. Compared with *in utero* injections, the method described here is less invasive to the mother, and the pup survival rate suggests it is well tolerated. Moreover, tissue damage using the adaptor should be lower than with freehand injections. The design takes advantage of conventional adult stereotaxic apparatuses and facilitates the implementation of neonatal intracerebral viral injections for any lab accustomed to adult mouse intracerebral injections. Because the adaptor is mounted directly on the ear and tooth bars, the new-

born head can be balanced on the stereotaxic frame, more closely approximating the adult condition. Hypothermia-induced anesthesia was chosen for its simplicity and effectiveness in newborn mouse pups; however, gas anesthesia has also been used successfully in pups, and the adaptor could be modified to fit the necessary tubing [11]. The neonatal adaptor best fits P0-1 C57BL/6 mice, but the 3D printer instructions (Supplementary data) can be modified for different head sizes, depending on the mouse strain. As demonstrated with two distinct *Cre* mouse lines, the neonatal stereotaxic adaptor is a valuable tool for members of the scientific community seeking to target small neuronal populations reliably in the early postnatal period.

## Supplementary data

To view the supplementary data that accompany this paper please visit the journal website at: [www.future-science.com/doi/suppl/10.2144/btn-2020-0050](http://www.future-science.com/doi/suppl/10.2144/btn-2020-0050)

## Author contributions

P Olivetti codedesigned the stereotaxic adaptor, performed stereotaxic surgeries and immunohistochemistry experiments, and wrote the manuscript. C Lacefield codedesigned and fabricated the stereotaxic adaptor (3D printing). C Kellendonk supervised design of the adaptor and experiment, and edited the manuscript.

## Acknowledgments

The authors would like to acknowledge Alexander Harris at Columbia University Department of Psychiatry for graciously granting access to the 3D printer used to fabricate the neonatal stereotaxic device.

## Financial & competing interests disclosure

P Olivetti: Leon Levy Fellowship in Neuroscience, NIMH T32 Research Fellowship (2T32MH018870 – 33; PI Jonathan Javitch). C Kellendonk: NIH R01 MH093672. The authors have no other relevant affiliations or financial involvement with any organization or entity with a financial interest in or financial conflict with the subject matter or materials discussed in the manuscript apart from those disclosed.

No writing assistance was utilized in the production of this manuscript.

## Ethical conduct of research

The experiments described in this report have been conducted according to the policies and ethical guidelines established by the institutional review boards at Columbia University and the New York State Psychiatric Institute. The Institutional Animal Care and Use Committee (IACUC) protocol number for the experiments described here is 1526 (Kellendonk). A total of 12 *Adora2a-Cre* and 8 *Dat-IRES-Cre* mice were used in the experiments described in this manuscript, as noted in the main text.

## Open access

This work is licensed under the Attribution-NonCommercial-NoDerivatives 4.0 Unported License. To view a copy of this license, visit <http://creativecommons.org/licenses/by-nc-nd/4.0/>

## References

Papers of special note have been highlighted as: ● of interest; ●● of considerable interest

1. Marin O. Developmental timing and critical windows for the treatment of psychiatric disorders. *Nat. Med.* 22(11), 1229–1238 (2016).
2. Lim L, Mi D, Llorca A, Marin O. Development and functional diversification of cortical interneurons. *Neuron* 100(2), 294–313 (2018).
3. Meredith RM. Sensitive and critical periods during neurotypical and aberrant neurodevelopment: a framework for neurodevelopmental disorders. *Neurosci. Biobehav. Rev.* 50, 180–188 (2015).
- Highlights the growing importance of understanding the role of sensitive and critical periods in the emergence of neurodevelopmental disorders.
4. Kozorovitskiy Y, Saunders A, Johnson CA, Lowell BB, Sabatini BL. Recurrent network activity drives striatal synaptogenesis. *Nature* 485(7400), 646–650 (2012).
5. Skilbeck KJ, Johnston GAR, Hinton T. Long-lasting effects of early-life intervention in mice on adulthood behaviour, GABAA receptor subunit expression and synaptic clustering. *Pharmacol. Res.* 128, 179–189 (2018).
6. Lieberman OJ, McGuirt AF, Mosharov EV *et al.* Dopamine triggers the maturation of striatal spiny projection neuron excitability during a critical period. *Neuron* 99(3), 540–554.e4 (2018).
7. Sheu J-R, Hsieh C-Y, Jayakumar T *et al.* A critical period for the development of schizophrenia-like pathology by aberrant postnatal neurogenesis. *Front. Neurosci.* 13, 635 (2019).
8. Davidson S, Truong H, Nakagawa Y, Giesler GJ. A microinjection technique for targeting regions of embryonic and neonatal mouse brain *in vivo*. *Brain Res.* 1307, 43–52 (2010).
- Used a hand-carved stage made of extruded polystyrene foam to inject viruses into neonatal mouse brains under a stereotaxic frame.
9. Cheatham CEJ, Grier BD, Belluscio L. Bulk regional viral injection in neonatal mice enables structural and functional interrogation of defined neuronal populations throughout targeted brain areas. *Front. Neural Circuits* 9, 72 (2015).
10. Chen S-Y, Kuo H-Y, Liu F-C. Stereotaxic surgery for genetic manipulation in striatal cells of neonatal mouse brains. *J. Vis. Exp.* 137, 57270 (2018).
- Used an adaptor built out of a micropipette tip box and the tip of a microtube to hold the mouse neonate under a stereotaxic frame.
11. He CX, Arroyo ED, Cantu DA, Goel A, Portera-Cailliau C. A versatile method for viral transfection of calcium indicators in the neonatal mouse brain. *Front. Neural Circuits* 12, 56 (2018).
- Detailed protocol for expressing calcium sensors in the neocortex of newborn mice by using gas anesthesia and a microdrill.
12. TinkerCAD. <http://www.tinkercad.com>
13. Paxinos G, Halliday GM, Watson C, Koutcherov Y, Wang H. *Atlas of the Developing Mouse Brain at E17.5, P0 and P6 (1st Edition)*. Academic Press, Elsevier, London, UK (2007).
14. Durieux PF, Schiffmann SN, de Kerchove d'Exaerde A. Targeting neuronal populations of the striatum. *Front. Neuroanat.* 5, 40 (2011).
15. Allen Institute for Brain Science. Allen developing mouse brain atlas. <http://developingmouse.brain-map.org/>

16. Lammel S, Steinberg EE, Földy C *et al.* Diversity of transgenic mouse models for selective targeting of midbrain dopamine neurons. *Neuron* 85(2), 429–438 (2015).
17. Block ER, Nuttle J, Balcita-Pedicino JJ *et al.* Brain region-specific trafficking of the dopamine transporter. *J. Neurosci.* 35(37), 12845–12858 (2015).
18. de la Rossa A, Jabaudon D. *In vivo* rapid gene delivery into postmitotic neocortical neurons using iontoporation. *Nat. Protoc.* 10(1), 25–32 (2015).
- Excellent illustration of the relationship between vascular lambda and skull suture lambda.
19. Rombo DM, Newton K, Nissen W *et al.* Synaptic mechanisms of adenosine A2A receptor-mediated hyperexcitability in the hippocampus. *Hippocampus* 25(5), 566–580 (2015).